Tribhuvan University Journal Vol. 41, No. 1 | pp. 188–205
Tribhuvan University • Kirtipur, Kathmandu, Nepal • ISSN 2091-0916 • Estd. 1964 Year: 2026

Original Research Article
DOI:10.3126/tuj.v41i1.92508

In Silico Molecular Docking and ADMET Evaluation of Bioactive Phytochemicals from *Urtica dioica* (Sisnu) as Potential Anti-Cancer Agents

Govind Bahadur Dhami[1,*], **Madhab Raj Bhatt**[2], **Shiv Raj Joshi**[3], **Bhawani Datt Joshi**[4]

[1]Shree Janata Secondary School, Sakayal, Dadeldhura, Nepal
[2]Shree Ghanteshwor Secondary School, Doti, Nepal
[3]Shree Janata Secondary School, Kanchanpur, Nepal
[4]Shree Siddhanath Science Campus, Mahendranagar, Tribhuvan University, Nepal
[*]*Correspondence:* dhami.gov@gmail.com

Article History

Received: 02 April, 2026 Revised: 28 June, 2026
Accepted: 28 June, 2026 Published: 30 June, 2026

How to Cite:

Dhami, G. B., Bhatt, M. R., Joshi, S. R., & Joshi, B. D. (2026). In silico molecular docking and ADMET evaluation of bioactive phytochemicals from *Urtica dioica* (Sisnu) as potential anti-cancer agents. *Tribhuvan University Journal*, *41*(1), 188–205. https://doi.org/10.3126/tuj.v41i1.92508

Keywords

ADMET analysis, Molecular docking, Quercetin, Scopoletin, Kaempferol, *Urtica dioica*

ABSTRACT

This study adopted in silico molecular docking and ADMET approach to investigate the therapeutic potential of bioactive phytochemicals named Quercetin, Scopoletin, and Kaempferol, from *Urtica dioica* (Sisnu) for anticancer activity against human receptor tyrosine kinase(PDB ID: 4RT7), Janus Kinase (JAK2; PDB ID: 3UGC), and MYC transcription factor (PDB ID: 1NKP). These compounds were chosen because Urtica dioica is traditionally used in anti-inflammatory, anticancer ethnomedicine, and reported bioactivity with a suitable molecular size for oral therapeutics. This study fills the gap by directly comparing their ADMET, toxicity, and docking in the same computational workflow. The physicochemical properties, pharmacokinetics, and drug-likeness properties were assessed by using the SwissADME web tool. ProTox 3.0 was used to predict the acute toxicity of the phytochemicals, and Auto Dock Vina was used to investigate the interactions. All three compounds showed an acceptable physicochemical profile, modest lipophilicity, favorable solubility, and full alignment with the five rules of Lipinski, compatible with efficient oral bioavailability. Scopoletin showed the most balanced ADME profile, while quercetin and kaempferol are better suited for non-CNS targets. Predicted toxicity was manageable for all three phytochemicals, with lower liabilities for scopoletin and kaempferol, though PAINS and Brenk alerts around the catechol motif in quercetin call for careful experimental validation and optimization. Docking showed favorable scores for quercetin and kaempferol against the receptor tyrosine kinase (9.5 to 9.8 kcalmol^{-1}) and Janus kinase 2 (9.0 kcalmol^{-1}). These in silico results indicate quercetin and kaempferol merit further investigation as RTK/JAK2-directed anticancer scaffolds, while scopoletin may offer an ADME-advantaged chemotype; experimental validation is required before therapeutic claims.

Introduction

In the recent era, medicinal herbs and their bioactive phytochemicals, which have a long-lasting role in medicine, are the focus of extensive pharmacological research, driven by growing awareness of their therapeutic potential for the treatment of a diverse array of illnesses because of their low toxicity, proven medicinal value and environmentally friendly character (Cimárová et al., 2023; Dhami et al., 2023; Paneru et al., 2024; Roy et al., 2022). *Urtica dioica* (Sisnu) is an ethnomedicinal plant widely distributed across temperate regions of the world and is highly beneficial and packed with nutritional value including a rich profile of phytochemicals, amino acids, and essential minerals (Nepal et al., 2020; Parente et al., 2025). These chemicals show a wide range of pharmacological activities with potent antioxidant, antiviral, immunomodulatory, antidiabetic, antihypertensive, antiobesity, anti-allergy, anti-asthma, anti-Alzheimer's, anti-inflammatory, antifungal, antibacterial and anticancer activity with good safety (Abi Sleiman et al., 2024; Aghababaei & Hadidi, 2023; Eity et al., 2024; Frent et al., 2024; Xiong et al., 2024).

This study focuses on the *in silico* ADMET and molecular docking screening of quercetin, scopoletin and kaempferol, three well-documented phytochemicals found in *Urtica dioica*. This study aims to evaluate and compare the physicochemical properties, lipophilicity, aqueous solubility, pharmacokinetics, drug-likeness, toxicity profile and medicinal chemistry profile of quercetin, scopoletin and kaempferol using the SwissADME web tool under the same workflow (Daina et al., 2017). Additionally, a molecular docking approach was adopted to study the binding interactions of the molecules using AutoDock Vina (Trott & Olson, 2010) with three important cancer-related proteins: 4RT7 (receptor tyrosine kinase) (Smith et al., 2015), 3UGC (Janus kinase 2) (Perner et al., 2019), and 1NKP (myelocytoma proto-oncogene protein, MYC transcription factor) (Nair & Burley, 2003), which are associated with several types of cancer (Esposito et al., 2019; Whitfield, 2024; Zacarías-Fluck et al., 2024). The optimized molecular structures of quercetin, scopoletin and kaempferol are presented in Figure 1.

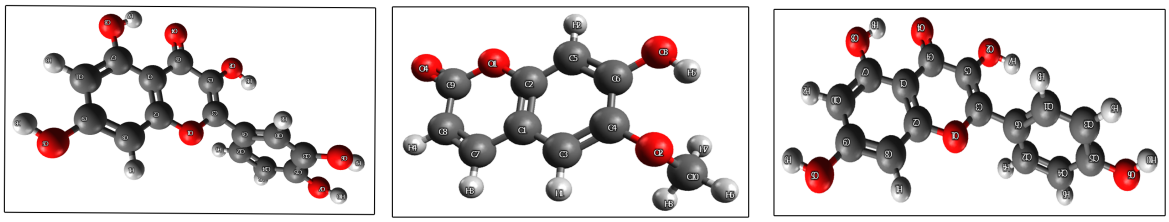

(a) (b) (c)

Figure 1
Optimized molecular structures of (a) quercetin, (b) scopoletin and (c) kaempferol with atom numbering (optimized using Avogadro).

Although a large array of bioactive phytochemicals contained in *Urtica dioica* are reported for their pharmacological activities, there is limited comparative *in silico* evidence on ADMET and molecular docking under the same workflow. Thus, it is difficult to recommend quercetin, kaempferol and scopoletin for further *in vivo* and *in vitro* validation without ADMET and molecular docking screening. The objectives of this study are as follows:

- To calculate and compare physicochemical properties, lipophilicity, aqueous solubility, pharmacokinetics, drug-likeness, and toxicity profiles of quercetin, scopoletin, and kaempferol using the SwissADME/ADMET web tools under the same workflow.
- To perform molecular docking of quercetin, scopoletin, and kaempferol against three cancer-related proteins with PDB IDs 4RT7, 3UGC, 1NKP using AutoDock Vina and compare binding affinities and key interactions.
- To combine ADMET and docking results to suggest which compound(s) show the most promising balance of drug-like properties and target binding for further experimental validation.

Given the global interest in low-toxicity therapeutics derived from plants and the extensive ethnomedicinal use of *Urtica dioica*, a systematic *in silico* comparison of its major phytochemicals will efficiently triage candidates for anticancer research. The ADMET and docking workflow on quercetin, scopoletin and kaempferol generates reproducible and cost-effective preliminary data to justify and focus future laboratory studies.

Literature review

The current search for new therapeutic treatments in the field of oncology is gradually turning towards investigation into natural products as potential candidates for powerful and safe therapeutic treatments (Abi Sleiman et al., 2024; Esposito et al., 2019). Among such plants, *Urtica dioica*, known for its ethnopharmacological properties, is a candidate which is scientifically recognized due to its abundant secondary metabolites which have demonstrated effective anti-proliferative and apoptosis induction in cancer cell lines (Esposito et al., 2019; Pant &

Sundriyal, 2016; Papang et al., 2025). Although traditional experimental pharmacology is capable of demonstrating the medicinal properties of extracts of *Urtica dioica*, their molecular interactions with target oncogenes are not fully known.

Recent studies have pointed out the possible medicinal uses of kaempferol (KMP), a flavonoid compound with a high level of anti-cancer activity through the prevention of cell proliferation, metastasis, and motility, and by inducing apoptosis (Amjad et al., 2022; de Morais et al., 2024; Felice et al., 2022; Imran et al., 2024; Sengupta et al., 2022). The ability of KMP to control molecular indicators and to stop the growth of blood vessels has revealed its potential to treat different solid malignancies and improve existing chemotherapy regimens. However, before using KMP in real practice, it is necessary to carry out additional research to solve the problems related to the low bioavailability of KMP and to set the correct doses of this drug.

The effectiveness of quercetin, which is one of the major dietary flavonoids, in treating cancer and acting as an antioxidant has been proven through consistent research. Some of the key discoveries regarding quercetin indicate that it stops tumor progression through cell cycle arrest, apoptosis, and metastasis, but targets only cancerous cells without affecting normal cells (Baghel et al., 2012; Maugeri et al., 2023; Tang et al., 2020). Other than this role, quercetin acts as a powerful antioxidant, which protects the body from free radicals and oxidative stress by regulating PI3K/AKT/mTOR and NF-κB signaling pathways (Biswas et al., 2022). Scopoletin is a natural coumarin with tremendous therapeutic potential. Research has demonstrated the effectiveness of scopoletin as an anticancer compound because of its ability to inhibit cancer growth by controlling cell cycle progression, apoptosis induction, and oncogenic signal transduction pathways (Gao et al., 2024; Meilawati et al., 2023). Although the substance has a non-toxic effect, the literature points out a number of pharmacokinetic problems (Antika et al., 2022).

The aim of this research is the *in silico* study of molecular docking in order to define the binding affinity of the selected bioactive phytochemicals of the plant on cancer-related receptors. Additionally, this research incorporates the *in silico* ADMET analysis and comparison in order to define the pharmacokinetics and toxicity of these phytochemicals under the same workflow.

Materials and Methods

Physicochemical properties, pharmacokinetics, drug-likeness, and medicinal chemistry

SwissADME web tool (http://www.swissadme.ch) (Daina et al., 2017) is utilized for prediction of physicochemical, pharmacokinetics, drug-likeness and medicinal chemistry properties. The canonical SMILES of quercetin, kaempferol and scopoletin were retrieved from PubChem (https://pubchem.ncbi.nlm.nih.gov/) and entered to the SwissADME web tool to generate the full set of data including significant physicochemical properties such as hydrogen bond donors and acceptors, molar refraction, polar surface area, rotatable bonds, and AlogP values and other relevant characteristics.

Molecular docking

Molecular docking studies were performed using AutoDock Vina (Trott & Olson, 2010), AutoDockTools (Morris et al., 2009), BIOVIA Discovery Studio (Dassault Systèmes, 2016), PyMOL (Schrödinger, LLC, 2020), Python, and Open Babel (O'Boyle et al., 2011). Docking proteins were retrieved from the RCSB Protein Data Bank (https://www.rcsb.org/) (Rose et al., 2011).

Protein structure preparation. Proteins were downloaded from the RCSB Protein Data Bank in PDB format. BIOVIA Discovery Studio and AutoDockTools were used to prepare them for the final docking purpose. Polar hydrogen atoms were accurately added to the target protein structure after the removal of all crystallographic water molecules and other unnecessary ligand molecules. Single chain (chain A) of 3UGC and 4RT7 were selected, and four chains A, B, D and E of 1NKP were prepared for the docking.

Ligand structure preparation. The ligands, quercetin, scopoletin and kaempferol, were downloaded from the PubChem database in SDF format and then converted to PDB format using Open Babel (O'Boyle et al., 2011). Ligands were optimized using Avogadro with Merck Molecular Force Field 1994 (MMFF94). AutoDockTools were used to prepare ligands for final docking purpose and saved in PDBQT format.

Grid construction for docking. The molecular docking technique was employed using blind docking, wherein the grid was designed optimally to cover the maximum possible binding sites of the protein. The active sites of the protein have been predicted by removing water molecules within a grid box of size 60 Å $\times$ 60 Å $\times$ 60 Å with a spacing of 0.375 Å, which was sufficient to cover the whole protein under study.

Docking parameters used in this study are summarized in Table 1.

Table 1
Docking parameters used in this study

Parameters	Used values
Protonation	Protonated at physiological pH (7.4)
Force field	Merck Molecular Force Field 1994 (MMFF94)
Partial charges (ligands)	Gasteiger charges
Protein charges	Kollman charges
Grid size	60 Å × 60 Å × 60 Å; sufficient to cover the target protein
Grid spacing	0.375 Å
Docking type	Blind docking
Exhaustiveness	8
Number of poses	9

Docking. The molecular docking was done by AutoDock Vina software upon successful generation of the receptor and ligand structures, together with the respective config files. The docking was done through the Vina executable under defined conditions for the exploration of possible binding modes and affinities of the selected molecules.

Docking programs generally use a scoring function, which can be seen as an attempt to approximate the standard chemical potentials of the system (Trott & Olson, 2010). The general functional form of the conformation-dependent part of the scoring function of AutoDock Vina is given as:

$$c = \sum_{i<j} f_{t_i t_j}(r_{ij}) \tag{1}$$

The interaction functions $f_{t_i t_j}$ are defined relative to the surface distance $d_{ij} = r_{ij} - R_{t_i} - R_{t_j}$ (Jain, 1996).

The scoring function for AutoDock Vina can be obtained using the following equation:

$$\begin{aligned}\Delta G_{\text{binding}} = {} & \Delta G_{\text{H-bond}} + \Delta G_{\text{hydrophobic}} + \Delta G_{\text{repulsion}} \\ & + \Delta G_{\text{gauss}} + \Delta G_{\text{AutoDock Vina score}}\end{aligned} \tag{2}$$

The binding affinity prediction by AutoDock Vina is obtained using a weighted sum of atomatom interaction energies between ligand and receptor atoms along with a penalty for ligand flexibility. The scoring function consists of attractive Gaussians, steric repulsion, hydrophobic interactions, hydrogen bonds, and a rotatable bond penalty (Trott & Olson, 2010).

Visualization and analysis. BIOVIA Discovery Studio and PyMOL were used to visualize the outputs obtained from Vina (Dassault Systèmes, 2016; Schrödinger, LLC, 2020).

Ligand efficiency and inhibition constant. Ligand efficiency using AutoDock Vina is calculated by:

$$\text{Ligand efficiency} = \frac{\Delta G}{N} \tag{3}$$

where ΔG is the docking score and N is the number of heavy atoms.

The inhibition constant is calculated by:

$$K_i = e^{\frac{\Delta G}{RT}} \tag{4}$$

where ΔG is the docking score, R is the universal gas constant and T is the absolute temperature.

Toxicity profile screening

Computation-assisted toxicity testing has become an indispensable part of the process of discovering drugs, providing fast and inexpensive assessments of the compound's toxicity profile, prioritizing safer candidate molecules and thereby reducing the number of animal experiments needed for dosage and toxicity testing (Roy et al., 2022). In this study, ProTox 3.0 was adopted to calculate the toxicity of the phytochemicals quercetin, scopoletin and kaempferol (Banerjee et al., 2024). ProTox 3.0 is based on an ensemble of 61 models that employ descriptors based on molecular similarities, fragment propensities, common molecular features, and fragment similarity-driven clustering cross-validation to predict various types of toxicities, such as acute toxicity, organ-specific toxicity, mechanistic toxicology, molecular initiating events, Tox21 pathway perturbation, and toxicological targets (Banerjee et al., 2024).

Results and Discussion

Physicochemical properties

All the phytochemicals quercetin, scopoletin and kaempferol found in *Urtica dioica* (Sisnu) were systematically characterized for physicochemical properties to obtain vital information regarding their structural, functional and stability-related characteristics. The major parameters corresponding to the title compounds calculated by the SwissADME web tool are shown in Table 2. These parameters are vital to understanding the compound's behavior with respect to its suitability for the desired applications.

Table 2
Physicochemical properties of quercetin, scopoletin and kaempferol

Properties	Quercetin	Scopoletin	Kaempferol
Formula	$C_{15}H_{10}O_7$	$C_{10}H_8O_4$	$C_{15}H_{10}O_6$
Molecular weight (g/mol)	302.24	192.17	286.24
Number of heavy atoms	22	14	21
Number of aromatic heavy atoms	16	10	16
Fraction Csp^3	0.00	0.10	0.00
Number of rotatable bonds	1	1	1
Number of H-bond acceptors	7	4	6
Number of H-bond donors	5	1	4
Molar refractivity	78.03	51.00	76.01
TPSA ($Å^2$)	131.136	59.67	111.13

The comparison of physicochemical profiles of quercetin, scopoletin and kaempferol evokes their relevance to the design of drugs and oral bioavailability. Among them, scopoletin shows the most favorable profile for oral bioavailability and membrane permeability, whereas quercetin and kaempferol are highly aromatic and polar, which may enhance target binding but limit solubility and membrane permeability.

Lipophilicity

Lipophilicity is the ability of a substance to bind to lipids (fats) and non-polar solvents. It is a crucial property of a compound since it influences the compound's behavior within the body, its capacity to cross cell membranes, and its interactions with biological targets. ADMET (absorption, distribution, metabolism, excretion, and toxicity) are directly related to lipophilicity (Klimoszek et al., 2024). The lipophilicity of quercetin, scopoletin and kaempferol is displayed in Table 3.

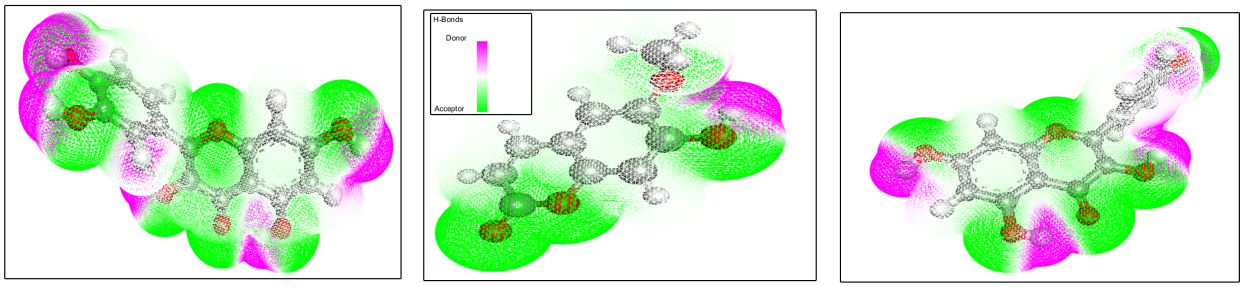

(a) (b) (c)

Figure 2
Hydrogen-bond acceptor and donor surface maps of (a) quercetin, (b) scopoletin and (c) kaempferol.

Table 3
Lipophilicity of quercetin, scopoletin and kaempferol

Properties	Quercetin	Scopoletin	Kaempferol
Log $P_{o/w}$ (iLOGP)	1.63	1.86	1.70
Log $P_{o/w}$ (XLOGP3)	1.54	1.53	1.90
Log $P_{o/w}$ (WLOGP)	1.99	1.51	2.28
Log $P_{o/w}$ (MLOGP)	-0.56	0.76	-0.03
Log $P_{o/w}$ (SILICOS-IT)	1.54	1.94	2.03
Consensus Log $P_{o/w}$	1.23	1.52	1.58

The computed values of $P_{o/w}$ from iLOGP, XLOGP3, WLOGP, MLOGP and SILICOS-IT indicate moderate lipophilicity for quercetin, scopoletin and kaempferol, with consensus values of 1.23, 1.52 and 1.58, respectively. Scopoletin and kaempferol possess a slightly higher overall lipophilicity profile than quercetin, especially in WLOGP and SILICOS-IT matrices, suggesting better membrane permeability potential and thus stronger interaction in lipid-rich targets.

Water solubility

The water solubility shows moderate to good solubility across all models. Water solubility of the title compounds is presented in Table 4. The solubility (log *S*) of the target molecules was implemented by three different models: ESOL (Delaney, 2004), Ali (Ali et al., 2012), and SILICOS-IT (Daina et al., 2017). Even though all compounds are classified as being soluble, the comparative analysis clearly shows that scopoletin is more soluble than quercetin, which in turn is more soluble than kaempferol with respect to their solubility in water. The

same trend holds for their lipophilicity, indicating that scopoletin has the best ratio of solubility and permeability, an important factor in determining drug-likeness and absorption through the oral route.

Table 4
Water solubility of quercetin, scopoletin and kaempferol

Water Solubility	Quercetin	Scopoletin	Kaempferol
Log *S* (ESOL)	-3.16	-2.46	-3.31
Solubility (ESOL)	0.211 mg/ml; 6.98×10^{-4} mol/l	0.67 mg/ml; 3.48×10^{-3} mol/l	0.140 mg/ml; 4.90×10^{-4} mol/l
Class (ESOL)	Soluble	Soluble	Soluble
Log *S* (Ali)	-3.91	-2.39	-3.86
Solubility (Ali)	0.0374 mg/ml; 1.24×10^{-4} mol/l	0.779 mg/ml; 4.06×10^{-3} mol/l	0.398 mg/ml; 1.39×10^{-4} mol/l
Class (Ali)	Soluble	Soluble	Soluble
Log *S* (SILICOS-IT)	-3.24	-3.17	-3.82
Solubility (SILICOS-IT)	0.173 mg/ml; 5.73×10^{-4} mol/l	0.131 mg/ml; 6.81×10^{-4} mol/l	0.0429 mg/ml; 1.50×10^{-4} mol/l
Class (SILICOS-IT)	Soluble	Soluble	Soluble

The solubility (log *S*) of the target molecules was implemented by three different models: ESOL (Delaney, 2004), Ali (Ali et al., 2012), and SILICOS-IT (Daina et al., 2017). Even though all compounds are classified as being soluble, the comparative analysis clearly shows that scopoletin is more soluble than quercetin, which in turn is more soluble than kaempferol with respect to their solubility in water. The same trend holds for their lipophilicity, indicating that scopoletin has the best ratio of solubility and permeability, an important factor in determining drug-likeness and absorption through the oral route.

Pharmacokinetics

Table 5 shows the pharmacokinetic properties of quercetin, scopoletin and kaempferol.

Table 5
Pharmacokinetics of quercetin, scopoletin and kaempferol

Pharmacokinet	Quercetin	Scopoletin	Kaempferol
GI absorption	High	High	High
BBB permeant	No	Yes	No
P-gp substrate	No	No	No
CYP1A2 inhibitor	Yes	Yes	Yes
CYP2C19 inhibitor	No	No	No
CYP2C9 inhibitor	No	No	No
CYP2D6 inhibitor	Yes	No	Yes
CYP3A4 inhibitor	Yes	No	Yes
Log K_p (skin permeation, cm/s)	-7.05	-6.39	-6.70

All the compounds show gastrointestinal absorption, which indicates efficient oral uptake. Quercetin and kaempferol are bloodbrain barrier (BBB) impenetrant, limiting central nervous system (CNS) penetration, whereas scopoletin does cross the BBB (Abbott, 2004). All are not expected to be refluxed by P-gp transporters because they are not substrates of P-glycoprotein. They inhibit CYP1A2 and do not inhibit CYP2C19 and CYP2C9, suggesting that they may interact with drugs metabolized by such enzymes. The lower value of Log K_p shows their lower skin permeation. Quercetin and kaempferol require caution as they inhibit CYP3A4 and CYP2D6 and could lead to toxic buildup of other prescribed drugs in a patient's system.

Drug-likeness

For a compound to be considered as a candidate drug for eventual use, it must possess optimal pharmacokinetics and safety characteristics and desired biological activity (Hu et al., 2018). The drug-likeness of the title compounds was evaluated by considering various parameters like molecular weight, hydrogen bond acceptor and donor, molar refractivity, polar surface area, rotatable bond number, and AlogP through the SwissADME web tool. The result is summarized in Table 6.

Lipinski's five rules are a widely recognized framework in drug discovery, providing necessary guidelines for initial classification of a drug candidate (Lipinski et al., 2001; Paneru et al., 2024). This framework helps to assess the potential of a compound in terms of oral bioavailability and serves as a fundamental tool for evaluating physicochemical properties, pharmacokinetics and overall suitability as a drug (Daina et al., 2017; Lipinski et al., 2001; Rizwana et al., 2020). Expected values for all of these criteria are listed in the last column of Table 6.

It turns out that all drug-like properties of quercetin, scopoletin and kaempferol meet the requirements of Lipinski's rule of five; therefore, these substances can be considered suitable for oral administration. A model of the BOILED-Egg model is given in Figure 3, while the bioavailability radar chart is provided in Supplementary Figure 1.

Table 6

Drug-likeness parameters of quercetin, scopoletin and kaempferol

Parameters	Quercetin	Scopoletin	Kaempferol	Range expected
Molecular weight (g/mol)	302.24	192.17	286.24	≤ 500
H-bond donors	5	1	4	≤ 5
H-bond acceptors	7	4	6	≤ 10
Number of rotatable bonds	1	1	1	≤ 10
Polar surface area (PSA, Å^2)	131.136	59.67	111.13	≤ 140
AlogP	1.99	1.51	2.28	≤ 5
Molar refractivity	78.03	51.00	76.01	40130
Lipinski	Yes; 0 violation	Yes; 0 violation	Yes; 0 violation	

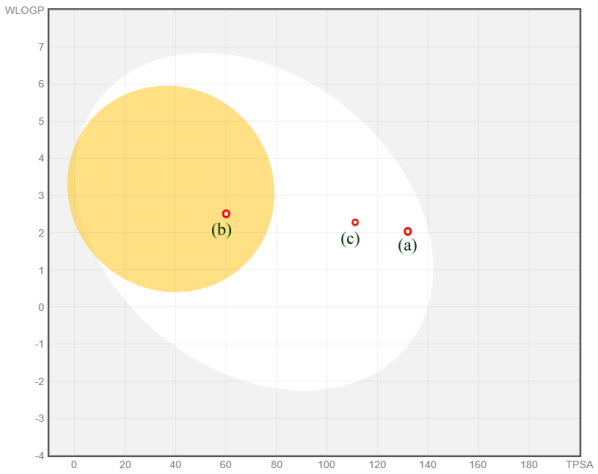

Figure 3

BOILED-Egg plots of (a) quercetin, (b) scopoletin, and (c) kaempferol showing predicted gastrointestinal absorption and blood–brain barrier penetration.

The compound located in the white region indicates good predicted human intestine absorption, which is favourable for oral administration, and that located inside the yolk suggests a higher probability of bloodbrain penetration and usefulness for CNS-targeted drugs. Among the three compounds, scopoletin is located within the yolk of the BOILED-Egg, indicating moderate WLOGP and TPSA values and a well-balanced lipophilicitypolarity profile, which is favorable for drug developability and bioavailability. In contrast, the remaining two phytochemicals fall outside the optimal regions, suggesting possible limitations in oral absorption and/or bloodbrain barrier penetration. This is because of high polarity and multiple hydroxyl groups, which reduce membrane permeability. They are better for non-CNS targets, local action, or optimization strategies such as prodrug design, nanoformulation, or structural modification to improve bioavailability.

The bioavailability radar chart generated by SwissADME is a hexagonal graph used to assess the drug-likeness of a molecule. It possesses six axes, each axes representing a key parameter lipophilicity (Daina et al., 2017; Ononamadu & Ibrahim, 2021), size, topological polar surface area, solubility, saturation (fraction of carbon in sp^3 hybridization) and flexibility. These parameters in combination provide a comprehensive evaluation of the compound's potential bioavailability and drug-likeness. The value of XLOGP3 should range from −0.7 to +5.0, size should be less or equal to 500 g/mol, TPSA should be less or equal to 140 Å^2, saturation should be at least 25% and the number of rotatable bonds no more than 10 allowed. Also, the title molecule showed 0 violations in Ghose (Ghose et al., 1999), Veber (Veber et al., 2002), Egan (Egan et al., 2000), and Muegge (Muegge et al., 2001) rules of 5 (RO5) screening. The bioavailability radar charts of (a) quercetin, (b) scopoletin and (c) kaempferol are represented in Supplementary Figure 1. Among them, scopoletin shows a balanced profile as it shows properties closest to the optimal range.

Medicinal chemistry

The medicinal chemistry investigation of the title compound raised one alert for PAINS (Pan-assay interference compound). Due to the presence of catechol A, it may lead to false positives in high-throughput screening assay. Likewise, a Brenk alert for catechol suggests metabolic instability. On the other hand, the title compound is classified as lead-like, suggesting favorable characteristics often seen in early-stage drug candidate in terms of size and functional diversity. The synthetic accessibility score of 3.23 suggests that its synthesis and production may have some sort of complexities. Conclusively, quercetin shows promise as a lead, PAINS and Brenk alerts point to potential challenge that cannot be neglected.

Toxicity profile

Toxicity of chemicals is the ability of a substance to cause harmful effects in biological systems, such as cells,

organs or whole organisms, leading to structural or functional damage. In drug design, toxicity screening is used to proactively identify potential hazards, avoid costly failures in later development stages, and ensure that a candidate drug is safe for human use (Sharma et al., 2017). In this study, ProTox 3.0 (Banerjee et al., 2024) was adopted to calculate the toxicity of the phytochemicals quercetin, scopoletin and kaempferol.

The toxicity radar plots of quercetin, kaempferol and scopoletin are shown in Supplementary Figure 6(a)–(c). The profiles suggest manageable toxicity with only a few moderate, target-specific liabilities that warrant focused experimental validation. The detailed toxicity profile of all three molecules is summarized in Table 7.

Table 7
Toxicity profile of quercetin, scopoletin and kaempferol predicted by ProTox 3.0

Target	Quercetin prediction	Quercetin probability	Scopoletin prediction	Scopoletin probability	Kaempferol prediction	Kaempferol probability
Hepatotoxicity	Inactive	0.69	Inactive	0.69	Inactive	0.68
Neurotoxicity	Inactive	0.89	Inactive	0.82	Inactive	0.89
Nephrotoxicity	Active	0.62	Active	0.64	Active	0.62
Respiratory toxicity	Active	0.83	Active	0.78	Active	0.83
Cardiotoxicity	Inactive	0.99	Inactive	0.61	Inactive	0.91
Carcinogenicity	Active	0.68	Active	0.53	Inactive	0.72
Immunotoxicity	Inactive	0.87	Active	0.54	Inactive	0.96
Mutagenicity	Active	0.51	Inactive	0.56	Inactive	0.52
Cytotoxicity	Inactive	0.99	Inactive	0.91	Inactive	0.98
BBB-barrier	Active	0.53	Active	0.58	Active	0.57
Ecotoxicity	Inactive	0.53	Inactive	0.54	Inactive	0.51
Clinical toxicity	Inactive	0.53	Active	0.51	Inactive	0.54
Nutritional toxicity	Active	0.63	Active	0.59	Active	0.66
Aryl hydrocarbon receptor (AhR)	Active	0.91	Active	0.51	Active	1.00
Androgen receptor (AR)	Inactive	0.99	Inactive	0.99	Inactive	0.99
Androgen receptor ligand binding domain (AR-LBD)	Inactive	0.97	Inactive	0.78	Inactive	0.99
Aromatase	Inactive	0.91	Inactive	0.89	Active	0.96
Estrogen receptor alpha (ER)	Active	0.87	Inactive	0.71	Active	1.00
Estrogen receptor ligand binding domain (ER-LBD)	Active	0.95	Inactive	0.70	Active	0.95
Peroxisome proliferator activated receptor gamma (PPAR-gamma)	Inactive	0.98	Inactive	0.95	Inactive	0.95
Nrf2/ARE (nuclear factor (erythroid-derived 2)-like 2 / antioxidant responsive element)	Inactive	0.99	Inactive	0.96	Inactive	0.99
Heat shock factor response element (HSE)	Inactive	0.99	Inactive	0.96	Inactive	0.99
Mitochondrial membrane potential (MMP)	Active	1.00	Inactive	0.53	Active	1.00
Phosphoprotein (tumor suppressor) p53	Inactive	0.97	Inactive	0.87	Inactive	0.92
ATPase family AAA domain-containing protein 5 (ATAD5)	Inactive	0.99	Inactive	0.75	Inactive	0.92
Thyroid hormone receptor alpha (THRα)	Inactive	0.90	Inactive	0.90	Inactive	0.90
Thyroid hormone receptor beta (THRβ)	Inactive	0.78	Inactive	0.78	Inactive	0.78
Transthyretin (TTR)	Inactive	0.97	Inactive	0.97	Inactive	0.97
Ryanodine receptor (RYR)	Inactive	0.98	Inactive	0.98	Inactive	0.98
GABA receptor (GABAR)	Inactive	0.96	Inactive	0.96	Inactive	0.96
Glutamate N-methyl-D-aspartate receptor (NMDAR)	Inactive	0.92	Inactive	0.92	Inactive	0.92

Target	Quercetin prediction	Quercetin probability	Scopoletin prediction	Scopoletin probability	Kaempferol prediction	Kaempferol probability
AMPAR (alpha-amino-3-hydroxy-5-methyl-4-isoxazolepropionate receptor)	Inactive	0.97	Inactive	0.97	Inactive	0.97
Kainate receptor (KAR)	Inactive	0.99	Inactive	0.99	Inactive	0.99
Acetylcholinesterase (AChE)	Inactive	0.69	Inactive	0.69	Inactive	0.68
Constitutive androstane receptor (CAR)	Inactive	0.98	Inactive	0.98	Inactive	0.98
Pregnane X receptor (PXR)	Inactive	0.92	Inactive	0.92	Inactive	0.92
NADH-quinone oxidoreductase (NADHOX)	Inactive	0.97	Inactive	0.97	Inactive	0.97
Voltage-gated sodium channel (VGSC)	Inactive	0.95	Inactive	0.95	Inactive	0.95
Na^+/I^- symporter (NIS)	Inactive	0.98	Inactive	0.98	Inactive	0.98
Cytochrome CYP1A2	Active	1.00	Inactive	0.58	Active	0.93
Cytochrome CYP2C19	Active	0.77	Inactive	0.86	Active	0.65
Cytochrome CYP2C9	Active	0.99	Active	0.53	Active	0.66
Cytochrome CYP2D6	Inactive	0.85	Inactive	0.63	Active	0.62
Cytochrome CYP3A4	Inactive	0.79	Inactive	0.91	Inactive	0.65
Cytochrome CYP2E1	Inactive	1.00	Inactive	0.99	Inactive	1.00

Molecular docking

Molecular docking is a computer-based technique employed in predicting the way in which a drug molecule binds to a protein receptor (M. K. Chaudhary et al., 2020). It predicts binding modes as well as binding affinity of ligand with target proteins which plays a key role in drug design (M. Chaudhary & Tyagi, 2024; M. K. Chaudhary et al., 2020). This study attempts to analyze the inhibitory potency, binding interaction, and reactive site of three cancer-associated proteins. The proteins with code 4RT7, 3UGC and 1NKP were retrieved from the Protein Data Bank to conduct molecular docking with quercetin (Rose et al., 2011). The active sites for the proteins are predicted by removing the water molecules in the grid of dimensions 60 Å × 60 Å × 60 Å having spacing of 0.375 Å. Binding results from the estimations done using the AutoDock Vina program with various parameters of the docked structure of the ligand and chosen proteins are listed in Tables 8, 9 and 10. Binding of the ligands to proteins is related to their least binding affinity. AutoDock Vina gives nine different ligand binding mechanisms. The results of docking are interpreted in terms of conventional hydrogen bonding as they can specify complementary groups in protein binding sites and are responsible to influence the ligand's binding orientation by contributing overall binding affinity (Meyer et al., 1996). The structures of the proteins are displayed in Figure 4, while their Ramachandran plots are provided in Supplementary Figure 2.

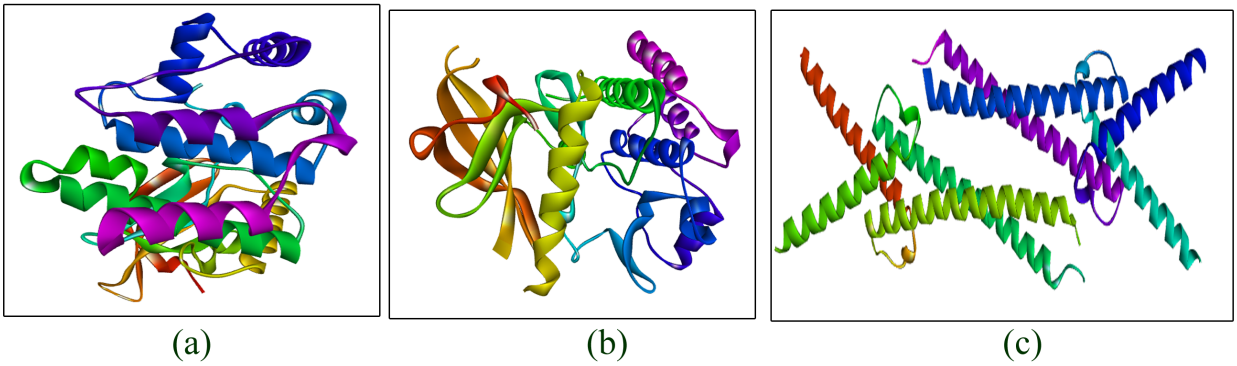

Figure 4
Three-dimensional structures of target proteins: 3UGC (a), 4RT7 (b), and 1NKP (c).

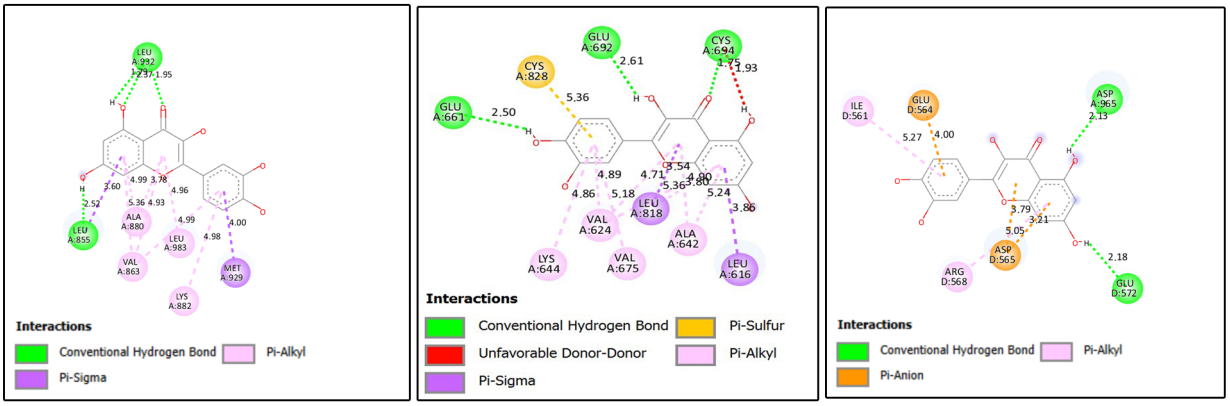

Figure 5

Two-dimensional protein–ligand interactions of quercetin docked with (a) 3UGC, (b) 4RT7 and (c) 1NKP.

The corresponding three-dimensional hydrogen-bonding views are provided in Supplementary Figure 3.

4RT7 is known to mediate crucial intracellular signaling pathways involved in cellular functions like cell division, differentiation, and apoptosis. Receptor tyrosine kinases can be mutated or dysregulated, leading to uncontrolled cellular proliferation and changes implicated in many cancers (Sangwan & Park, 2006). Janus kinase 2 is a non-receptor tyrosine kinase that plays a key role in signaling pathways of various cytokine receptors influencing immune function and hematopoiesis. Mutation, particularly V617F mutation, in JAK2 leads to uncontrolled cell proliferation (Perner et al., 2019). 1NKP belongs to MYC transcription factor which is a well-known oncogene implicated in various kinds of cancers (Whitfield, 2024; Zacarías-Fluck et al., 2024).

Docking result of quercetin with 3UGC, 4RT7 and 1NKP. Quercetin docked against 4RT7, 3UGC, and 1NKP, as presented in Table 8. In the case of 4RT7, a grid box centered around $x = -40.601400$, $y = 11.239975$, and $z = -13.827825$ was set up and Vina with an exhaustiveness of 8. Docking score was observed at -9.5 kcal/mol with an inhibition constant of 0.107 μM and a ligand efficiency of -0.41. RMSD l.b. and RMSD u.b. were measured as 0.00 Å, and hydrogen bonding occurred between GLU A:661, GLU A:692, and CYS A:694 through atoms H31, H28, and O8 with bond lengths of 2.50, 2.61 and 1.75 Å, respectively, which are within the acceptable range, where 1.75 Å is the HůůA distance rather than conventional hydrogen bond (Chen & Kurgan, 2009; Ippolito et al., 1990; van Bergen et al., 2016).

For 3UGC, a grid box was set up to be centered at $x = 19.985585$, $y = -18.075829$ and $z = -17.863171$ with the same exhaustiveness. The complex exhibited a binding energy of -9.0 kcal/mol, an inhibition constant of 0.249 μM, a ligand efficiency of -0.43, and an RMSD of 0.00 Å. Hydrogen bonds were noted for LEU A:932, LEU A:855, ASP A:965, and GLU B:572 with distances between atoms O4, O8, H29, H30, H31, and H32 being 2.37 Å, 1.95 Å, 1.79 Å, 2.52 Å, 2.13 Å and 2.18 Å. The calculated bond lengths are within acceptable range (Hubbard & Haider, 2010).

The grid box centered at $x = 53.729491$, $y = 47.972001$, and $z = 57.669586$ coordinates was found to contain the active sites for the 1NKP protein. The ligand binds to the protein with the affinity of -7.6 kcal/mol ($K_i = 2.648$ μM) and ligand efficiency of -0.35. There are two hydrogen bonds that help to stabilize the complex: ASP A:965H29 (2.13 Å) and GLU D:572H30 (2.18 Å).

The two-dimensional protein–ligand interaction views of quercetin with the proteins 3UGC, 4RT7 and 1NKP are displayed in Figure 5. Three-dimensional hydrogen-bonding views of quercetin docked with the selected proteins are presented in Supplementary Figure 3.

Quercetin showed good binding with the three targets in a favorable manner by forming a network of traditional hydrogen bonding and hydrophobic interactions. Out of the three complexes, 4RT7 formed the most number of interactions, while 3UGC and 1NKP formed lesser but significant interactions, which denote stable binding of the ligand in their pockets.

Docking result of kaempferol with 3UGC, 4RT7 and 1NKP. Docking studies were carried out by placing kaempferol into the active site using the grid center values for 3UGC (19.985585, -18.075829, -17.863171), 4RT7 (-40.601400, 11.239975, -13.827825) and 1NKP (53.729491, 47.972001, 57.669586) with exhaustiveness = 8. From Table 9, it can be observed that 4RT7 shows the maximum binding energy of -9.8 kcal/mol, while 3UGC shows -9.0 kcal/mol. Figure 6 shows the two dimensional protein ligand interaction of docking of kaempferol with the proteins 3UGC, 4RT7 and 1NKP. Kaempferol had positive binding interactions with all the three proteins due to hydrogen bonding and non-covalent interactions. 4RT7 had the most number of interaction sites, while 3UGC and 1NKP had fewer but stable interaction sites. Three dimensional view of H-Bonding of docking of kaempferol with the respective proteins is presented in the supplementary figure 4.

Table 8
Docking result (quercetin)

Selected PDB code and their resolution	Binding affinity (kcal/mol)	H-bond residues	Atoms	Bond length h (Å)	Ligand efficiency	Inhibition constant (μM)	RMSD l.b. (Å)	RMSD u.b. (Å)
4RT7 (3.1 Å) (receptor tyrosine kinase)	-9.5	GLU A:661	H31	2.50	-0.43	0.107	0.00	0.00
		GLU A:692	H28	1.75				
		CYS A:694	O4	2.61				
3UGC (1.34 Å) (Janus kinase 2)	-9.0	LEU A:932	O4	2.37	-0.41	0.249	0.00	0.00
		LEU A:932	O8	1.95				
		LEU A:855	H29	1.79				
		ASP A:965	H30	2.52				
		GLU B:572	H31	2.13				
		GLU B:572	H32	2.18				
1NKP (1.80 Å) (MYC, transcription factor)	-7.6	ASP A:965	H29	2.13	-0.35	2.648	0.00	0.00
		GLU D:572	H30	2.18				

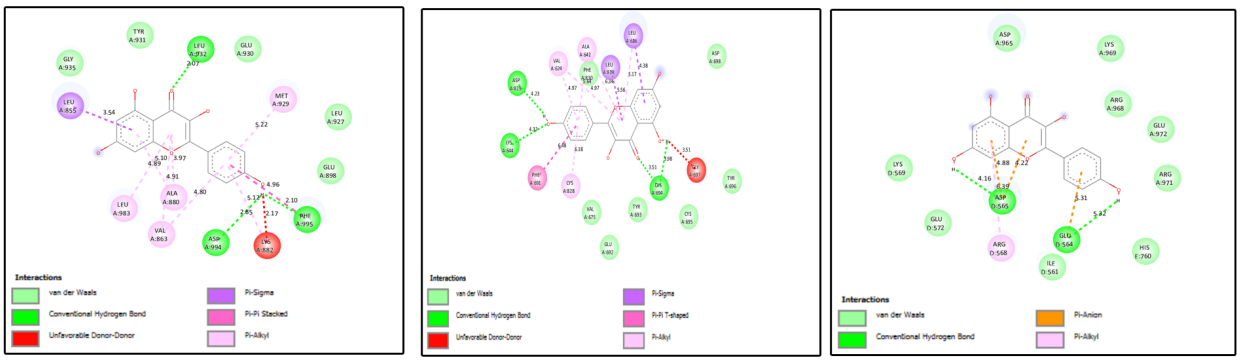

Figure 6
Two-dimensional protein–ligand interactions of kaempferol docked with (a) 3UGC, (b) 4RT7 and (c) 1NKP.

The corresponding three-dimensional hydrogen-bonding views are provided in Supplementary Figure 4.

Docking result of scopoletin with 3UGC, 4RT7 and 1NKP. Active binding sites of proteins 3UGC, 4RT7 and 1NKP were confirmed within a grid box, centered at (19.985585, −18.075829, −17.863171), (−40.601400, 11.239975, −13.827825) and (53.729491, 47.972001, 57.669586) respectively. Docking results are shown in Table 10, while the docked structures with their 2D interactions are illustrated in Figure 7. Scopoletin showed moderate interaction with the proteins under investigation, with a docking energy of −7.2 kcal/mol (3UGC), −7.3 kcal/mol (4RT7) and −5.7 kcal/mol (1NKP).

The two-dimensional protein–ligand interaction views of scopoletin with the proteins 3UGC, 4RT7 and 1NKP are displayed in Figure 7, and the three-dimensional hydrogen-bonding views of scopoletin docked with the respective proteins are shown in Supplementary Figure 5.

The interactions between scopoletin and proteins 3UGC, 4RT7, and 1NKP were achieved via hydrogen bonding and hydrophobicity interactions mediated by pi (π). Different interaction modes were observed in the three protein structures; however, protein 4RT7 had more diverse types of interaction than proteins 3UGC and 1NKP.

Table 9
Docking result (kaempferol)

Selected PDB code and resolution	Binding affinity (kcal/mol)	H-bond residues	Atoms	Bond length (Å)	Ligand efficiency	Inhibition constant (μM)	RMSD l.b./u.b. (Å)
4RT7 (3.1 Å) (receptor tyrosine kinase)	-9.8	LYS A:644	O9	2.37	-0.46	0.064	0.00 / 0.00
		ASP A:829	H6	2.73			
		CYS A:694	O4	1.95			
		CYS A:694	H10	1.83			
3UGC (1.34 Å) (Janus kinase 2)	-9.0	LEU A:932	O4	2.07	-0.42	0.25	0.00 / 0.00
		ASP A:994	H10	2.85			
		PHE A:995	H10	2.10			
1NKP (1.80 Å) (MYC, transcription factor)	-7.3	GLU D:564	H10	2.68	-0.34	4.40	0.00 / 0.00
		ASP D:565	H6	2.44			

Table 10
Docking result (scopoletin)

Selected PDB code and their resolution	Binding affinity (kcal/mol)	H-bond residues	Atoms	Bond length (Å)	Ligand efficiency	Inhibition constant (μM)	RMSD l.b. (Å)	RMSD u.b. (Å)
4RT7 (3.1 Å) (receptor tyrosine kinase)	-7.2	CYS A:694	O8	2.18	-0.51	5.3	0.00	0.00
3UGC (1.34 Å) (Janus kinase 2)	-7.3	LEU A:932	O8	1.98	-0.52	4.4	0.00	0.00
1NKP (1.80 Å) (MYC, transcription factor)	-5.7				0.40	66	0.00	0.00

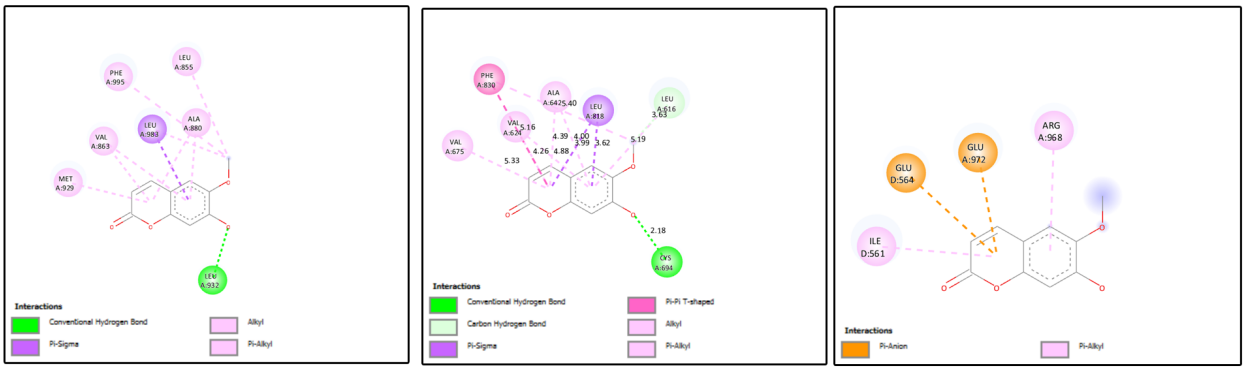

Figure 7
Two-dimensional protein–ligand interactions of scopoletin docked with (a) 3UGC, (b) 4RT7 and (c) 1NKP.

The corresponding three-dimensional hydrogen-bonding views are provided in Supplementary Figure 5.

Conclusion

In silico screening of quercetin, scopoletin and kaempferol from *Urtica dioica* reveals that all three phytochemicals possess acceptable physicochemical profiles, moderate lipophilicity, good aqueous solubility and full alignment with Lipinski's rule of five, supporting their suitability as orally bioavailable molecules (Daina et al., 2017). Among them, scopoletin shows the most balanced ADME profile, with optimal TPSA, lipophilicity, solubility and BOILED-Egg positioning, indicating good membrane permeability, intestinal absorption and blood–brain barrier penetration, while quercetin and kaempferol remain better suited for non-CNS targets due to higher polarity and multiple hydrogen-bonding functionalities (Daina et al., 2017). Toxicity profiles screened by ProTox 3.0 reveal manageable safety liabilities for all three phytochemicals, with scopoletin and kaempferol showing comparatively lower predicted toxicity than quercetin, although the PAINS and Brenk alerts for the catechol motif in quercetin underline the need for careful validation and structural optimization before progression (Banerjee et al., 2024).

Molecular docking screening against cancer associated targets 4RT7 (RTK), 3UGC (JAK2) and 1NKP (MYC) indicates that quercetin and kaempferol competitively bind to the pockets of 4RT7 and 3UGC for scoring functions up to 9.8 kcal/mol alongside predicted inhibitory values in the submicromolar range due to hydrogen bonding interactions with them, as well as favorable ligand efficiencies, while scopoletin is weakly bound to these three proteins. Quercetin and kaempferol emerge as attractive lead-like chemical classes against RTKs/JAK2 targets, whereas scopoletin serves as a drug-like chemical class that favors ADME properties and can be suggested for CNS-based multi-target therapies. This needs to be validated by molecular dynamics studies, free energy calculations, and pharmacological studies.

Implications

The above-mentioned computational results demonstrate that quercetin, kaempferol, and scopoletin from *Urtica dioica* (*Sisnu*) have good physicochemical properties, pharmacokinetics, and toxicity, as well as favorable interactions with certain cancer targets. Specifically, the affinity of quercetin and kaempferol to receptor tyrosine kinase and JAK2 indicates the necessity of conducting further biological research concerning these phytochemicals. Nevertheless, these results only represent computational predictions without any evidence of therapeutic potential, so no conclusions can be made regarding their possible use as an anti-cancer medication without any valid validation.

Further research should include validation of these results via in vitro and in vivo tests. Molecular dynamic simulations and free-energy calculations will be able to confirm the stability of complexes between ligands and proteins. The analysis of structural activity relationships and modification of these phytochemicals will be able to enhance their biological activity.

Supplementary Figures

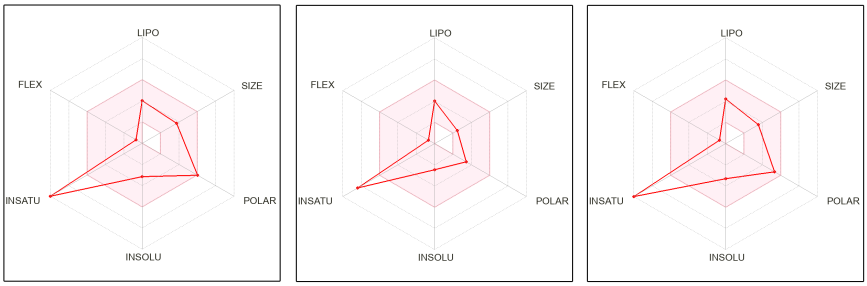

(a) (b) (c)

Supplementary Figure 1

Bioavailability radar charts of (a) quercetin, (b) scopoletin and (c) kaempferol.

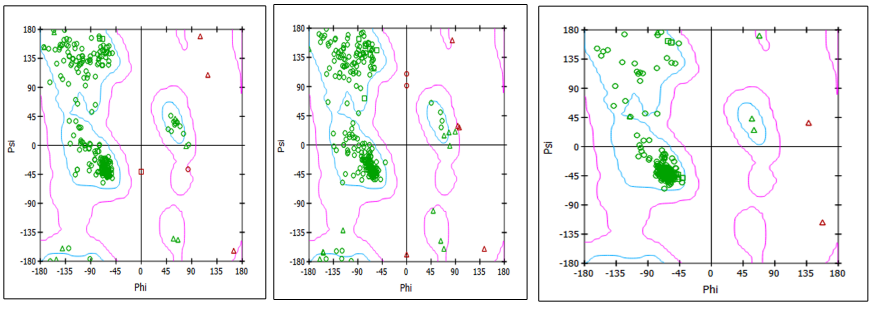

(a) (b) (c)

Supplementary Figure 2

Ramachandran plots of proteins (a) 3UGC, (b) 4RT7 and (c) 1NKP.

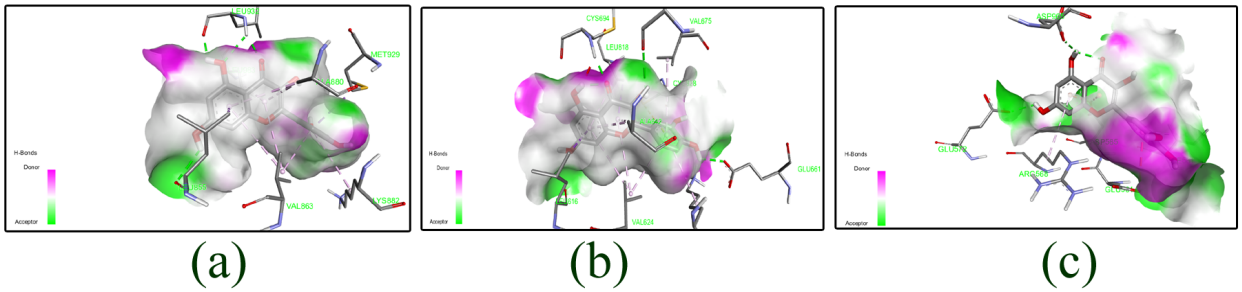

Supplementary Figure 3
Three-dimensional hydrogen-bonding views of quercetin docked with (a) 3UGC, (b) 4RT7 and (c) 1NKP.

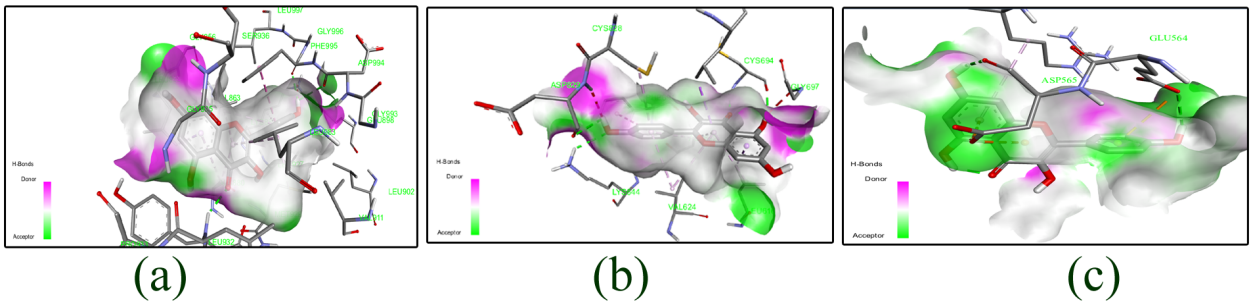

Supplementary Figure 4
Three-dimensional hydrogen-bonding views of kaempferol docked with (a) 3UGC, (b) 4RT7 and (c) 1NKP.

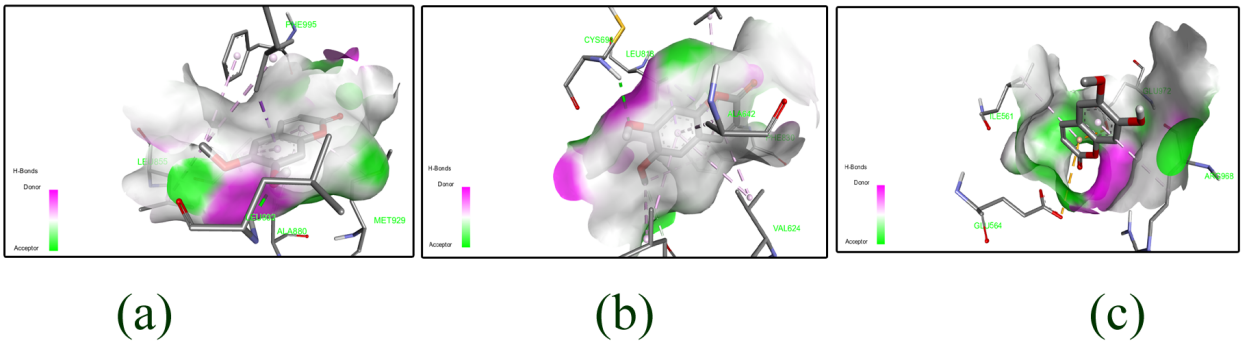

Supplementary Figure 5
Three-dimensional hydrogen-bonding views of scopoletin docked with (a) 3UGC, (b) 4RT7 and (c) 1NKP.

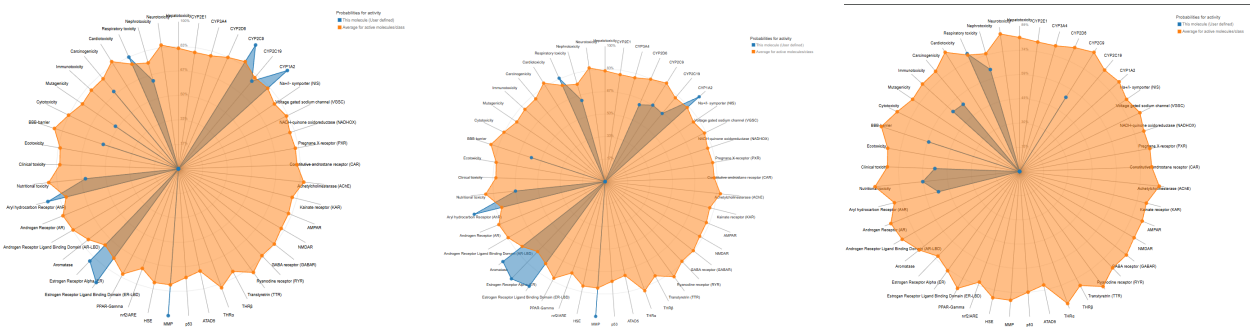

Supplementary Figure 6
Toxicity radar charts of (a) quercetin, (b) kaempferol and (c) scopoletin.

Authors' contribution

G. B. Dhami performed the molecular docking studies and prepared the manuscript. M. R. Bhatt contributed to data interpretation and assisted in manuscript preparation. S. R. Joshi carried out the toxicity prediction and its analysis. B. D. Joshi conceived and supervised the study and extracted and analyzed the SwissADME data. All authors reviewed and approved the final version of the manuscript.

Acknowledgments

The authors express their gratitude to the developers of SwissADME, ProTox-3.0, AutoDock Vina, PyMOL, and BIOVIA Discovery Studio for providing freely accessible computational resources that facilitated this study. The authors also thank their respective institutions for providing academic support and a conducive research environment.

Artificial Intelligence (AI) use and disclosure

In the preparation of this manuscript, artificial intelligence (AI) tools were used to assist with language editing and formatting for some sections, with subsequent human review and minimal or no modification of the scientific content.

Similarity and originality confirmation

The authors confirm that this manuscript is original, has not been published previously, is not under review elsewhere, and complies with the publication ethics and policies of the *Tribhuvan University Journal*.

Funding

No external funding was received for the conduct of this research or for the preparation of this manuscript.

Conflict of interest

The authors declare that they have no conflicts of interest related to this work.

Data availability

The datasets generated and analyzed during the current study are available from the corresponding author upon reasonable request.

References

Abbott, N. J. (2004). Prediction of blood–brain barrier permeability in drug discovery from *In Vivo*, *In Vitro* and *In Silico* models. *Drug Discovery Today: Technologies*, *1*(4), 407–416. https://doi.org/10.1016/j.ddtec.2004.11.014

Abi Sleiman, M., Younes, M., Hajj, R., Salameh, T., Abi Rached, S., Abi Younes, R., Daoud, L., Doumiati, J. L., Frem, F., Ishak, R., Medawar, C., Naim, H. Y., & Rizk, S. (2024). *Urtica dioica*: Anticancer properties and other systemic health benefits from *In Vitro* to clinical trials. *International Journal of Molecular Sciences*, *25*(13), 7501. https://doi.org/10.3390/ijms25137501

Aghababaei, F., & Hadidi, M. (2023). Recent advances in potential health benefits of quercetin. *Pharmaceuticals*, *16*, 1020. https://doi.org/10.3390/ph16071020

Ali, J., Camilleri, P., Brown, M. B., Hutt, A. J., & Kirton, S. B. (2012). Revisiting the general solubility equation: *In Silico* prediction of aqueous solubility incorporating the effect of topographical polar surface area. *Journal of Chemical Information and Modeling*, *52*, 420–428. https://doi.org/10.1021/ci200387c

Amjad, E., Sokouti, B., & Asnaashari, S. (2022). A systematic review of anti-cancer roles and mechanisms of kaempferol as a natural compound. *Cancer Cell International*, *22*, 260. https://doi.org/10.1186/s12935-022-02673-0

Antika, L. D., Tasfiyati, A. N., Hikmat, H., & Septama, A. W. (2022). Scopoletin: A review of its source, biosynthesis, methods of extraction, and pharmacological activities. *Zeitschrift für Naturforschung C*, *77*, 303–316. https://doi.org/10.1515/znc-2021-0193

Baghel, S. S., Shrivastava, N., Baghel, R. S., Agrawal, P., & Rajput, S. (2012). A review of quercetin: Antioxidant and anticancer properties. *World Journal of Pharmacy and Pharmaceutical Sciences*, *1*, 146–160.

Banerjee, P., Kemmler, E., Dunkel, M., & Preissner, R. (2024). ProTox 3.0: A webserver for the prediction of toxicity of chemicals. *Nucleic Acids Research*, *52*(W1), W513–W520. https://doi.org/10.1093/nar/gkae303

Biswas, P., Dey, D., Biswas, P. K., Rahaman, T. I., Saha, S., Parvez, A., Khan, D. A., Lily, N. J., Saha, K., Sohel, M., Hasan, M. M., Al Azad, S., Bibi, S., Hasan, M. N., Rahmatullah, M., Chun, J., Rahman, M. A., & Kim, B. (2022). A comprehensive analysis and anti-cancer activities of quercetin in ROS-mediated cancer and cancer stem cells. *International Journal of Molecular Sciences*, *23*, 11746. https://doi.org/10.3390/ijms231911746

Chaudhary, M., & Tyagi, K. (2024). A review on molecular docking and its application. *International Journal of Advanced Research*, *12*(3), 1141–1153. https://doi.org/10.21474/IJAR01/18505

Chaudhary, M. K., Srivastava, A., Singh, A. K., Tandon, P., & Joshi, B. D. (2020). Computational evaluation of molecular stability, reactivity, and drug potential of frovatriptan from DFT and molecular docking approach. *Computational and Theoretical Chemistry*, *1191*, 113031. https://doi.org/10.1016/j.comptc.2020.113031

Chen, K., & Kurgan, L. (2009). Investigation of atomic level patterns in protein-small ligand interactions. *PLoS ONE*, *4*(2), e4473. https://doi.org/10.1371/journal.pone.0004473

Cimárová, B., Hubková, B., Tomeková, V., & Birková, A. (2023). Flavonoids as promising natural compounds in the prevention and treatment of selected skin diseases. *International Journal of Molecular Sciences*, *24*, 6324. https://doi.org/10.3390/ijms24076324

Daina, A., Michielin, O., & Zoete, V. (2017). SwissADME: A free web tool to evaluate pharmacokinetics, drug-likeness and medicinal chemistry friendliness of small molecules. *Scientific Reports*, *7*, 42717. https://doi.org/10.1038/srep42717

Dassault Systèmes. (2016). *BIOVIA discovery studio*.

de Morais, E. F., de Oliveira, L. Q. R., Farias Morais, H. G., Souto Medeiros, M. R., de Almeida Freitas, R., Rodini, C. O., & Coletta, R. D. (2024). The anticancer potential of kaempferol: A systematic review based on *In Vitro* studies. *Cancers*, *16*, 585. https://doi.org/10.3390/cancers16030585

Delaney, J. S. (2004). ESOL: Estimating aqueous solubility directly from molecular structure. *Journal of Chemical Information and Computer Sciences*, *44*(3), 1000–1005. https://doi.org/10.1021/ci034243x

Dhami, G. B., Bhatt, M. R., Joshi, S. R., & Joshi, B. D. (2023). First principle study on structural, electronic, vibrational properties and molecular docking study of tyramine. *KMC Journal*, *5*(1), 241–260. https://doi.org/10.3126/kmcj.v5i2.58241

Egan, W. J., Merz, K. M., & Baldwin, J. J. (2000). Prediction of drug absorption using multivariate statistics. *Journal of Medicinal Chemistry*, *43*, 3867–3877. https://doi.org/10.1021/jm000292e

Eity, T. A., Bhuia, M. S., Chowdhury, R., Ahmmed, S., Salehin, S., Akter, R., & Islam, M. T. (2024). Therapeutic efficacy of quercetin and its nanoformulation both as mono- or combination therapies in the management of cancer: An update with molecular mechanisms. *Journal of Tropical Medicine*, *2024*(1), 5594462. https://doi.org/10.1155/2024/5594462

Esposito, S., Bianco, A., Russo, R., Di Maro, A., Isernia, C., & Pedone, P. V. (2019). Therapeutic perspectives of molecules from *Urtica dioica* extracts for cancer treatment. *Molecules*, *24*(15), 2753. https://doi.org/10.3390/molecules24152753

Felice, M. R., Maugeri, A., De Sarro, G., Navarra, M., & Barreca, D. (2022). Molecular pathways involved in the anti-cancer activity of flavonols: A focus on myricetin and kaempferol. *International Journal of Molecular Sciences*, *23*, 4411. https://doi.org/10.3390/ijms23084411

Frent, O. D., Stefan, L., Morgovan, C. M., Duteanu, N., Dejeu, I. L., Marian, E., Vicas, L., & Manole, F. (2024). A systematic review: Quercetin—secondary metabolite of the flavonol class, with multiple health benefits and low bioavailability. *International Journal of Molecular Sciences*, *25*, 12091. https://doi.org/10.3390/ijms252212091

Gao, X.-Y., Li, X.-Y., Zhang, C.-Y., & Bai, C.-Y. (2024). Scopoletin: A review of its pharmacology, pharmacokinetics, and toxicity. *Frontiers in Pharmacology*, *15*, 1268464. https://doi.org/10.3389/fphar.2024.1268464

Ghose, A. K., Viswanadhan, V. N., & Wendoloski, J. J. (1999). A knowledge-based approach in designing combinatorial or medicinal chemistry libraries for drug discovery: A qualitative and quantitative characterization of known drug databases. *Journal of Combinatorial Chemistry*, *1*, 55–68. https://doi.org/10.1021/cc9800071

Hu, Q., Feng, M.-L., Lai, L.-M., & Pei, J. (2018). Prediction of drug-likeness using deep autoencoder neural networks. *Frontiers in Genetics*, *9*, 585. https://doi.org/10.3389/fgene.2018.00585

Hubbard, R. E., & Haider, M. K. (2010). Hydrogen bonds in proteins: Role and strength. In *Encyclopedia of life sciences*. John Wiley & Sons. https://doi.org/10.1002/9780470015902.a0003011.pub2

Imran, M., Salehi, B., Sharifi-Rad, J., Gondal, T. A., Saeed, F., Imran, A., Shahbaz, M., Fokou, P. V. T., Arshad, M. U., Khan, H., Guerreiro, S. G., Martins, N., & Estevinho, L. M. (2024). Kaempferol: A key emphasis to its anticancer potential. *Molecules*, *29*, 2946. https://doi.org/10.3390/molecules29010001

Ippolito, J. A., Alexander, R. S., & Christianson, D. W. (1990). Hydrogen bond stereochemistry in protein structure and function. *Journal of Molecular Biology*, *215*, 457–471. https://doi.org/10.1016/S0022-2836(05)80364-X

Jain, A. N. (1996). Scoring noncovalent protein–ligand interactions: A continuous differentiable function tuned to compute binding affinities. *Journal of Computer-Aided Molecular Design*, *10*, 427–440. https://doi.org/10.1007/BF00124474

Klimoszek, D., Jele, M., Doowy, M., & Morak-Modawska, B. (2024). Study of the lipophilicity and ADMET parameters of new anticancer diquinothiazines with pharmacophore substituents. *Pharmaceuticals*, *17*, 725. https://doi.org/10.3390/ph17060725

Lipinski, C. A., Lombardo, F., Dominy, B. W., & Feeney, P. J. (2001). Experimental and computational approaches to estimate solubility and permeability in drug discovery and development settings. *Advanced Drug Delivery Reviews*, *46*(1–3), 3–26. https://doi.org/10.1016/S0169-409X(00)00129-0

Maugeri, A., Calderaro, A., Patanè, G. T., Navarra, M., Barreca, D., Cirmi, S., & Felice, M. R. (2023). Targets involved in the anti-cancer activity of quercetin in breast, colorectal and liver neoplasms. *International Journal of Molecular Sciences*, *24*, 2952. https://doi.org/10.3390/ijms24032952

Meilawati, L., Dewi, R. M., Tasfiyati, A. N., Septama, A. W., & Antika, L. D. (2023). Scopoletin: Anticancer potential and mechanism of action. *Asian Pacific Journal of Tropical Biomedicine*, *13*, 1–8. https://doi.org/10.4103/2221-1691.367685

Meyer, M., Wilson, P., & Schomburg, D. (1996). Hydrogen bonding and molecular surface shape complementarity as a basis for protein docking. *Journal of Molecular Biology*, *264*, 199–210. https://doi.org/10.1006/jmbi.1996.0634

Morris, G. M., Huey, R., Lindstrom, W., Sanner, M. F., Belew, R. K., Goodsell, D. S., & Olson, A. J. (2009). AutoDock4 and AutoDockTools4: Automated docking with selective receptor flexibility. *Journal of Computational Chemistry*, *30*(16), 2785–2791. https://doi.org/10.1002/jcc.21256

Muegge, I., Heald, S. L., & Brittelli, D. (2001). Simple selection criteria for drug-like chemical matter. *Journal of Medicinal Chemistry*, *44*, 1841–1846. https://doi.org/10.1021/jm015507e

Nair, S. K., & Burley, S. K. (2003). X-ray structures of Myc–Max and Mad–Max recognizing DNA: Molecular bases of regulation by proto-oncogenic transcription factors. *Cell*, *112*(2), 193–205. https://doi.org/10.1016/S0092-8674(02)01284-9

Nepal, M., Shrestha, S., Koirala, N., Paudel, P., & Adhikari, A. (2020). Phytochemical screening, antioxidant and anti-inflammatory activities of *Urtica dioica* L. from nepal. *Journal of Pharmacognosy and Phytochemistry*, *9*(5), 1123–1129.

O'Boyle, N. M., Banck, M., James, C. A., Morley, C., Vandermeersch, T., & Hutchison, G. R. (2011). Open babel: An open chemical toolbox. *Journal of Cheminformatics*, *3*, 33. https://doi.org/10.1186/1758-2946-3-33

Ononamadu, C. J., & Ibrahim, A. (2021). Molecular docking and prediction of ADME/drug-likeness properties of potentially active antidiabetic compounds isolated from aqueous-methanol extracts of *Gymnema sylvestre* and *Combretum micranthum*. *BioTechnologia*, *102*(1), 85–99. https://doi.org/10.5114/bta.2021.103765

Paneru, T. R., Chaudhary, M. K., Tandon, P., Chaudhary, T., & Joshi, B. D. (2024). Theoretical study on molecular stability, reactivity, and drug potential of cirsilineol from DFT and molecular docking methods. *Chemical Physics Impact*, *8*, 100641. https://doi.org/10.1016/j.chphi.2024.100641

Pant, V., & Sundriyal, R. C. (2016). Nutritional and therapeutic efficacy of stinging nettle: A review. *Journal of Ethnobiology and Traditional Medicine*, *126*, 1240–1254.

Papang, S. B., Kuotsu, K., Pradhan, S., Timsina, J., Sharma, S., & Bhattacharjee, A. (2025). Pharmacological properties and therapeutic potential of *Urtica dioica*: A comprehensive review. *Journal of Pharmaceutical Research*, *24*(3), 138–145. https://doi.org/10.18579/jopcr/v24.13.49

Parente, R., Paiva-Santos, A. C., Cabral, C., & Costa, G. (2025). Comprehensive review of *Urtica dioica* L. (Urticaceae) phytochemistry and anti-inflammatory properties. *Phytochemistry Reviews*, *24*, 1591–1628. https://doi.org/10.1007/s11101-024-09980-6

Perner, F., Perner, C., Ernst, T., & Heidel, F. H. (2019). Roles of JAK2 in aging, inflammation, hematopoiesis and malignant transformation. *Cells*, *8*(8), 854. https://doi.org/10.3390/cells8080854

Rizwana, B. F., Prasana, J. C. S., Muthu, & Abraham, C. S. (2020). Vibrational spectroscopy, reactive site analysis and molecular docking studies on 2-[(2-amino-6-oxo-6,9-dihydro-3*H*-purin-9-yl) methoxy]-3-hydroxypropyl (2*S*)-2-amino-3-methylbutanoate. *Journal of Molecular Structure*, *1202*, 127274. https://doi.org/10.1016/j.molstruc.2019.127274

Rose, P. W., Beran, B., Bluhm, W. F., Bi, C., Dimitropoulos, D., Goodsell, D. S., Prli, A., Quesada, M., Quinn, G. B., Westbrook, J. D., Young, J., Yukich, B., Zardecki, C., Berman, H. M., & Bourne, P. E. (2011). The RCSB protein data bank: Redesigned web site and web services. *Nucleic Acids Research*, *39*(Database issue), D392–D401. https://doi.org/10.1093/nar/gkq1021

Roy, A., Khan, A., Ahmad, I., Alghamdi, S., Rajab, B. S., Babalghith, A. O., Alshahrani, M. Y., Islam, S., & Islam, M. R. (2022). Flavonoids: A bioactive compound from medicinal plants and its therapeutic applications. *BioMed Research International*, *2022*(1), 5445291. https://doi.org/10.1155/2022/5445291

Sangwan, V., & Park, M. (2006). Receptor tyrosine kinases: Role in cancer progression. *Current Oncology*, *13*(5), 191–193. https://doi.org/10.3390/curroncol13050019

Schrödinger, LLC. (2020). *The PyMOL molecular graphics system* (Version 2.5.4). New York, NY.

Sengupta, B., Biswas, P., Roy, D., Lovett, J., Simington, L., Fry, D. R., & Travis, K. (2022). Anticancer properties of kaempferol on cellular signaling pathways. *Current Topics in Medicinal Chemistry*, *22*, 2474–2482. https://doi.org/10.2174/1568026622666220907112822

Sharma, A. K., Srivastava, G. N., Roy, A., & Sharma, V. K. (2017). ToxiM: A toxicity prediction tool for small molecules developed using machine learning and chemoinformatics approaches. *Frontiers in Pharmacology*, *8*, 880. https://doi.org/10.3389/fphar.2017.00880

Smith, C. C., Zhang, C., Lin, K. C., Lasater, E. A., Zhang, Y., Massi, E., Damon, L. E., Pendleton, M., Bashir, A., Sebra, R., Perl, A., Kasarskis, A., Shellooe, R., Tsang, G., Carias, H., Powell, B., Burton, E. A., Matusow, B., Zhang, J., & Shah, N. P. (2015). Characterizing and overriding the structural mechanism of the quizartinib-resistant FLT3 "gatekeeper" F691L mutation with PLX3397. *Cancer Discovery*, *5*(6), 668–679. https://doi.org/10.1158/2159-8290.CD-15-0060

Tang, S.-M., Deng, X.-T., Zhou, J., Li, Q.-P., Ge, X.-X., Miao, L., & Zhang, X.-Y. (2020). Pharmacological basis and new insights of quercetin action in respect to its anti-cancer effects. *Biomedicine & Pharmacotherapy*, *121*, 109604. https://doi.org/10.1016/j.biopha.2019.109604

Trott, O., & Olson, A. J. (2010). AutoDock Vina: Improving the speed and accuracy of docking with a new scoring function, efficient optimization, and multithreading. *Journal of Computational Chemistry*, *31*(2), 455–461. https://doi.org/10.1002/jcc.21334

van Bergen, L. A. H., Alonso, M., Palló, A., Nilsson, L., De Proft, F., & Messens, J. (2016). Revisiting sulfur H-bonds in proteins: The example of peroxiredoxin AhpE. *Scientific Reports*, *6*, 30369. https://doi.org/10.1038/srep30369

Veber, D. F., Johnson, S. R., Cheng, H.-Y., Smith, B. R., Ward, K. W., & Kopple, K. D. (2002). Molecular properties that influence the oral bioavailability of drug candidates. *Journal of Medicinal Chemistry*, *45*(12), 2615–2623. https://doi.org/10.1021/jm020017n

Whitfield, J. R. (2024). Editorial: MYC as a disease target beyond cancer. *Frontiers in Cell and Developmental Biology*, *12*, 1467372. https://doi.org/10.3389/fcell.2024.1467372

Xiong, F., Zhang, Y., Li, T., Tang, Y., Song, S.-Y., Zhou, Q., & Wang, Y. (2024). A detailed overview of quercetin: Implications for cell death and liver fibrosis mechanisms. *Frontiers in Pharmacology*, *15*, 1389179. https://doi.org/10.3389/fphar.2024.1389179

Zacarías-Fluck, M. F., Soucek, L., & Whitfield, J. R. (2024). MYC: There is more to it than cancer. *Frontiers in Cell and Developmental Biology*, *12*, 1342872. https://doi.org/10.3389/fcell.2024.1342872

Tribhuvan University Journal (TUJ) ISSN 2091-0916 • Estd. 1964

Tribhuvan University, Kirtipur, Kathmandu, Nepal nepjol.info/index.php/TUJ